Arch. Pharm. Res. (2020) 43:257–270
https://doi.org/10.1007/s12272-019-01202-4

Online ISSN 1976-3786
Print ISSN 0253-6269

Archives of Pharmacal Research
www.springer.com/12272

RESEARCH ARTICLE

Tizoxanide induces autophagy by inhibiting PI3K/Akt/mTOR pathway in RAW264.7 macrophage cells

Jiaoqin Shou[1,2] · Mi Wang[1] · Xiaolei Cheng[1] · Xiaoyang Wang[1] · Lifang Zhang[1] · Yingchun Liu[1] · Chenzhong Fei[1] · Chunmei Wang[1] · Feng Gu[1] · Feiqun Xue[1] · Juan Li[2] · Keyu Zhang[1]

Received: 21 June 2019 / Accepted: 6 December 2019 / Published online: 1 January 2020

Abstract As the main metabolite of nitazoxanide, tizoxanide (TIZ) has a broad-spectrum anti-infective effect against parasites, bacteria, and virus. In this study, we investigated the effects of TIZ on autophagy by regulating the PI3K/Akt/mTOR signaling pathway. RAW264.7 macrophage cells were treated with various TIZ concentrations. Cell viability assay, transmission electron microscope, and immunofluorescence staining were used to detect the biological function of the macrophage cells, and the expression levels of the autophagy pathway-related proteins were measured by Western blot. Results revealed that TIZ promoted the conversion of LC3-I to LC3-II, the formation of autophagy vacuoles, and the degradation of SQSTM1/p62 in a concentration- and time-dependent manner in RAW264.7 cells. Treatment with TIZ increased the Beclin-1 expression level and inhibited PI3K, Akt, mTOR, and ULK1 activation. These effects were enhanced by pretreatment with rapamycin but attenuated by pretreatment with LY294002. In addition, the conversion of LC3-I to LC3-II was observed in Vero, 293T, and HepG2 cells treated with TIZ. These data suggested that TIZ may induce autophagy by inhibiting the Akt/mTOR/ULK1 signaling pathway in macrophages and other cells.

✉ Juan Li
juanli@xtu.edu.cn

✉ Keyu Zhang
zcole@shvri.ac.cn

[1] Key Laboratory of Veterinary Chemical Drugs and Pharmaceutics, Ministry of Agriculture and Rural Affairs, Shanghai Veterinary Research Institute, Chinese Academy of Agricultural Sciences, 518 Ziyue RD, Minhang District, Shanghai 200241, China

[2] College of Chemistry, Xiangtan University, Yuhu District, Xiangtan 411105, Hunan, China

Keywords Autophagy · Tizoxanide · RAW264.7 cells · PI3K · mTOR

Introduction

Tizoxanide (TIZ, Fig. 1a) and nitazoxanide (NTZ, Fig. 1b) are synthetic thiazolide derivative that are developed as cestocidal agents as discovered by Rossignol (Somvanshi et al. 2014). NTZ has been licensed for the treatment of *Criptosporidium parvum* and *Giardia intestinalis* infections in nonimmunodeficient children and adults in the USA since 2002 and was marketed by Romark Laboratories under the trade name Alinia® (Fox and Saravolatz 2005; Rossignol et al. 2009; Stachulski et al. 2011). NTZ and TIZ also show broad activity against numerous parasitic and microbial pathogens (Dubreuil et al. 1996; Fox and Saravolatz 2005; Stachulski et al. 2017). Specifically, TIZ is more active than metronidazole against the metronidazole-susceptible isolates of *G. intestinalis* and resistant isolates (Adagu et al. 2002). The effectiveness of NTZ or TIZ against various viruses, such as rotavirus, influenza, norovirus, human immunodeficiency virus, respiratory syncytial virus, and hepatitis B and C viruses, in vitro and in vivo have been discovered and piqued the attention of scholars (Rossignol et al. 2009; Stachulski et al. 2011; La Frazia et al. 2013; Rossignol 2014; Belardo et al. 2015). Given the wide spectrum of pathogens targeted by NTZ and TIZ, thiazolides might possess other pharmacological properties and complex molecular actions.

Autophagy is an evolutionarily conserved and tightly regulated degradation system for intracellular components, which ultimately results in lysosomal digestion within mature cytoplasmic compartments (Essick and Sam 2010; Kobayashi 2015). At least three forms, including chaperone-mediated autophagy, microautophagy, and macroautophagy, have been identified. Macroautophagy is the major regulated catabolic

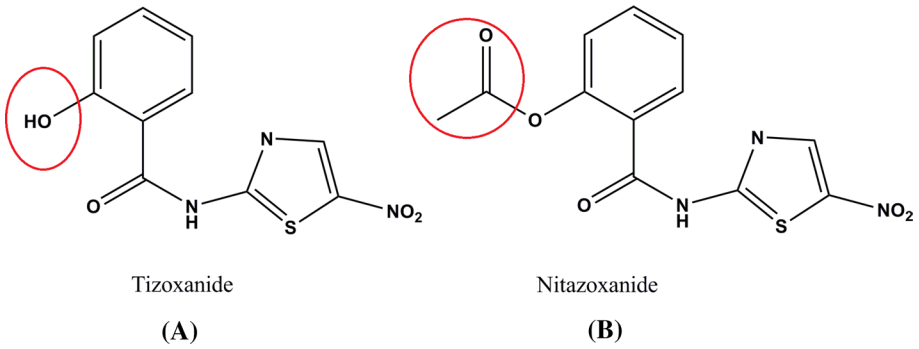

Fig. 1 Chemical structures of TIZ (**a**) and NTZ (**b**). The differences with a proton for TIZ and an acetyl moiety for NTZ show in circles

mechanism that eukaryotic cells use to degrade long-lived proteins and organelles (Levine and Kroemer 2008). Autophagy is involved in diverse physiological functions, including survival, differentiation, development, and homeostasis and protects organisms against diverse pathologies, including infections, cancer, and neurodegeneration (Levine and Kroemer 2008; Sparrer et al. 2017). Metformin, chloroquine, and rapamycin exert their pharmacological activities by participating in the autophagy of cells and regulating the related proteins (Kimura et al. 2013; Sotthibundhu et al. 2016; Wu et al. 2019).

In vivo, NTZ undergoes rapid deacetylation in plasma (half-life of 6 min) to form its metabolite TIZ, a compound with equal effectiveness, which is the only active form in the circulation unchanged even when plasma is diluted ten times (Adagu et al. 2002; Stockis et al. 2002a). Hence, NTZ is the active prodrug of TIZ, which is at least as active as NTZ against parasite, anaerobes, and viruses (Stockis et al. 2002b; Fox and Saravolatz 2005; Lam et al. 2012).

TIZ exerts anti-inflammatory effects by suppressing the activation of NF-κB and MAPK signaling pathways (Shou et al. 2019b). Autophagy is a key negative regulator of inflammation (Zhang et al. 2017). Compared with the wealth of information about TIZ against numerous pathogens or inflammatory, our knowledge about the role of TIZ in autophagy is still undeveloped. Here, TIZ was found to trigger autophagy in a concentration- and time-dependent manner. We further identified that the PI3K/Akt/mTOR pathway play important roles in the autophagy of RAW264.7 macrophage cells.

Materials and methods

Chemicals and reagents

TIZ (purity > 99.0%) and NTZ (purity > 98.5%) were synthesized by the Key Laboratory of Veterinary Chemical Drugs and Pharmaceutics, Ministry of Agriculture and Rural Affairs, Shanghai Veterinary Research Institute, Chinese Academy of Agricultural Sciences and characterized by LC–UV, LC–MS, and NMR methods. NTZ and TIZ were dissolving in DMSO at the concentrations of 200 and 100 mM, respectively, and stored at − 20 °C. Rabbit polyclonal anti-PI3K (#4257), anti-p-PI3K (#4228), anti-Akt (#4691), anti-p-Akt (#13,038), anti-mTOR (#2983), anti-p-mTOR (#5536), anti-ULK1 (#8054), anti-p-ULK1 (#14,202), anti-p62 (#23,214), anti-LC3 (#2775), and mouse polyclonal anti-β-actin (#3700) were purchased from Cell Signaling Technology (Beverly, MA, USA). HRP-coupled anti-rabbit and anti-mouse secondary antibodies were purchased from Abcam Inc. (Cambridge, MA, USA). Alexa Fluor488 goat anti-rabbit secondary antibody was purchased from Beyotime Biotechnology, Inc. (Shanghai, China). Lipopolysaccharide (LPS), LY294002, Rapamycin, and DMSO were purchased from Sigma-Aldrich (St. Louis, MO, USA). Fetal bovine serum (FBS) and Dulbecco's modified Eagle's medium (DMEM) were purchased from Gibco (Aukland, NZ). Polyvinylidene difluoride (PVDF) membrane, 4′,6-diamidino-2-phenylindole dihydrochloride (DAPI), BCA protein assay kit, and cell counting kit-8 (CCK-8) kit were purchased from Beyotime Biotechnology, Inc. (Shanghai, China). The ECL reagent (SuperSignal™ West Pico PLUS Chemiluminescent Substrate) was purchased from Thermo Fisher Scientific (Rockford, IL, USA). All other chemicals were of the highest grade commercially available.

Cell culture

RAW264.7, Vero, HepG2, and 293T cells were obtained from the cell bank of the Chinese Academy of Science (Shanghai, China). The cells were grown to 25 cm^2 flasks supplemented with DMEM complete medium containing 10% (v/v) heat-inactivated FBS. The cells were incubated at 37 °C in a humidified atmosphere of 5% CO_2 in air, and the medium was refreshed every 2–3 days. Under normal conditions, the shape of the cells was irregular round, with good refractive power and clear edges.

Cell viability assay

Cell viability was assessed using CCK-8 kit assay. The RAW264.7 cells were seeded in 96-well culture plates at a density of 5×10^4 cells/mL in 100 μL of medium and incubated for 12 h at 37 °C in the dark. Subsequently, the cells were

incubated with various TIZ or NTZ concentrations in 37 °C and 5% CO_2 incubator for 12 h. The cells were rinsed gently once by phosphate-buffered saline (PBS), and then cell culture medium containing 10% 0.5 mg/mL CCK-8 reagent was added into each well for 30 min incubation away from light. The absorbance of each well was measured at 450 nm using an Infinite M1000 PRO plate reader (TECAN, Austria). The results were reported in percentage with the vehicle control (the DMSO concentration in each group was 0.1%). The data are shown as the average of the five wells for each group. Each experiment was repeated three times. The viability of Vero, HepG2 and 293T cells treated with TIZ was also determined.

Transmission electron microscopy (TEM) examination

Autophagy can be observed by visualizing the ultrastructural features of the autophagic vesicles in cells by TEM (Ylä-Anttila et al. 2009). The RAW264.7 cells were rinsed with ice-cold 0.1 M PBS (pH of 7.4) and centrifuged at 500 × g for 5 min at room temperature, after which the clear supernatants were removed. Cell pellets were fixed with 2.5% glutaraldehyde at least 30 min at 4 °C. After fixation, the treated cells were thoroughly washed in PBS and then post-fixed with 1% OsO_4 for 1 h at room temperature. The cells were dehydrated in a graded series of ethanol and embedded in epoxy resin, and polymerization was then performed at 80 °C for 24 h. Blocks were cut on a Leica ultramicrotome into ultrathin sections (70 nm), which were post-stained with uranyl acetate and lead citrate and then viewed with a Tecnai G2 Spirit BIOTWIN TEM (FEI, Holland).

Immunofluorescence staining

The RAW264.7 cells were plated in six-well plates at a density of 2×10^5 cells/mL and then subjected to different experimental treatments, including 0, 25, 50, 75, and 100 μM TIZ. The cells were washed with sterile PBS two times, fixed with 4% paraformaldehyde in PBS for 20 min at room temperature, permeabilized with 0.1% Triton X-100 in PBS for 10 min, and washed with PBS three times. The cells were then blocked with 3% bovine serum albumin (BSA) for 60 min at room temperature and incubated with anti-LC3 antibody (dilution at 1:500) overnight at 4 °C. The cells were washed two times with PBS and incubated with Alexa Fluor488-conjugated secondary antibody at a dilution of 1:500 for 1 h in the dark. The nuclei were stained with DAPI for 10 min at room temperature in the dark. The cells were washed two times with PBS and viewed by a laser-scanning confocal microscope (Zeiss, LSM880, Germany).

Western blot analysis

The cells were seeded into six-well plates for further cultivation. After the confluence of the RAW264.7 cells reached 80–90%, the cells were subjected to different experimental treatments. After being collected and washed two times with ice-cold PBS (pH of 7.4), the cells were lysed with ice-cold RIPA buffer on ice for 15 min and harvested and collected via centrifugation at 12,000 × g for 10 min at 4 °C. The supernatants were stored at − 80 °C and further employed to determine protein concentration by using BCA protein assay (Beyotime Biotech Inc., China). Equal amounts of each total protein lysate (30 μg) were determined, mixed with 5 × SDS sample buffer, boiled for 5 min, and separated on a 10–15% SDS–polyacrylamide gel electrophoresis and then transferred onto immunoblot PVDF membranes at 250 mÅ. The blots were blocked at room temperature for 2 h in blocking buffer containing 5% BSA with Tris-buffered saline containing 0.1% Tween 20. The blots were incubated with primary antibodies against LC3B, p62, PI3K, p-PI3K, mTOR, p-mTOR, Akt, p-Akt, ULK1, p-ULK1, Atg7, Atg12, Beclin-1, and β-actin at 4 °C overnight. All primary antibodies were diluted at 1:1000. The membranes were washed three times with TBST for 10 min each time, incubated with a 1:5000 dilution of horseradish peroxidase-conjugated secondary antibodies at room temperature for 1 h, and washed again for three times with TBST. The immune complexes were detected by enhanced chemiluminescence reagents. The experiment was independently conducted for three times.

Intracellular ROS detection

Intracellular ROS was measured with the oxidation-sensitive fluorescent probe (DCFH-DA) as previously described (Li et al. 2006). RAW264.7 murine macrophages were seeded into 6-well plates with 12 h of cultivation. After being treated with 1 μg/mL LPS and 0, 25, 50, 75, and 100 μM TIZ in the culture medium for 6 h and treated with 75 μM TIZ for different times, the cells were washed two times with PBS. The macrophages were then incubated with 10 μM DCFH-DA at 37 °C for 20 min according to the manufacturer's instructions. DCFH-DA was deacetylated intracellularly by nonspecific esterase, which was further oxidized by ROS to the fluorescent compound 2,7-dichlorofluorescein (DCF). DCF fluorescence was detected by CytoFLEX flow cytometer (Becton Dickinson). For each sample, 10,000 events were collected.

Statistical analysis

All experiments were performed at least three times to ensure reproducibility. All values were showed as mean ± S.D. Statistical analysis was performed with SPSS 22.0 software. The significance of the differences was evaluated by one-way ANOVA. $P < 0.05$ was considered significant.

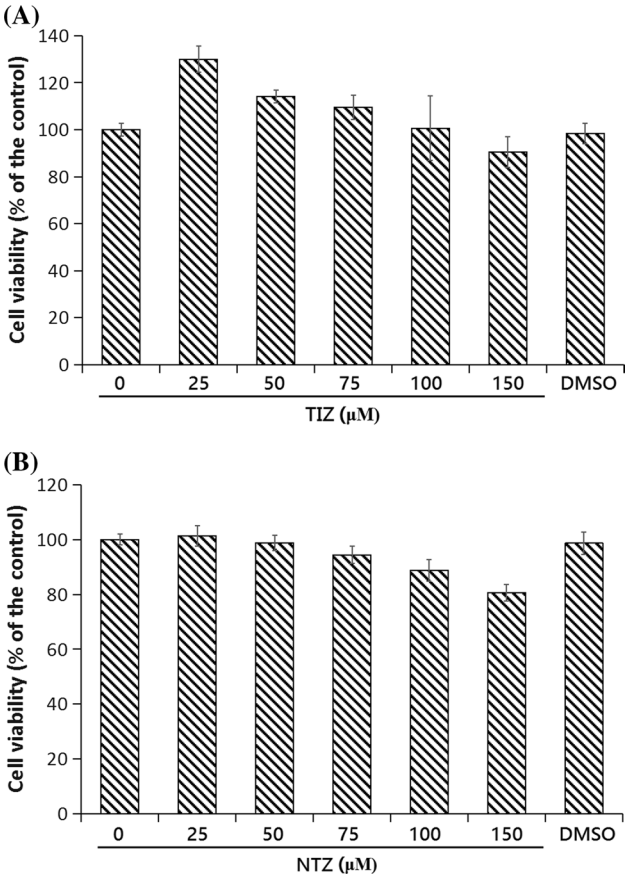

Fig. 2 Cytotoxicity of TIZ (**a**) and NTZ (**b**) on RAW264.7 cells. Cells were treated with TIZ at 25, 50, 75, 100, and 150 μM for 12 h, and cell viability was assayed by the CCK-8 kit. The cell viability of macrophage treated with NTZ and TIZ at 150 μM were resulted in significant decrease (90.43% and 80.65%, respectively). Data are expressed as the means ± S.D. of three independent experiments

Results

Effects of NTZ and TIZ on cell viability

RAW264.7 cells were exposed to different doses (0, 25, 50, 75, 100, and 150 μM) of NTZ and TIZ for 12 h to analyze the viability of these drugs on these cells. These cells were then cultured with these treatments and assayed for subsequent experiments. As shown in Fig. 2, NTZ and TIZ induced a cytotoxic effect on RAW264.7 cells in a dose-dependent manner. Compared with that of the control group, the viability of RAW264.7 cells was not significantly reduced when the NTZ and TIZ concentrations reached up to 100 μM. However, after the treatment with NTZ or TIZ at 150 μM, the cell viability of the macrophage significantly decreased (90.43% and 80.65%, respectively). The Vero, HepG2, and 293T cells were slightly more sensitive to TIZ than the RAW264.7 cells according to the cell viability analysis (data were not shown). Therefore, the doses of drug for further experiments were no more than 100 μM.

Immunofluorescence staining and TEM analysis

Immunofluorescence staining, TEM, and Western blot analysis were conducted to explore whether TIZ can induce autophagy in the RAW264.7 cells. As shown in Fig. 3a, the pattern of LC3 immunoreactivity was absent in the control cells. Immunofluorescence results exhibited that typical cytoplasmic LC3 punctate was formed considerably in the RAW264.7 cells exposed to TIZ, and LC3-labeled aggregation and the number of the cells with LC3-punctated foci significantly increased in a dose-dependent manner, thereby indicating that TIZ induced excessive autophagy of the RAW264.7 cells. As shown in Fig. 3b and c, a dose-dependent increase in the LC3-II/LC3-I expression level ratio in experimental groups was detected by Western blot ($P < 0.01$), which was in accordance with the results above. Western blot analysis (Fig. 3e and f) also revealed a time-dependent increase with 75 μM TIZ treatment in the LC3-II/LC3-I expression level ratio ($P < 0.01$). Compared with those of the control group, the LC3-II/LC3-I expression level ratios significantly increased by 72%, 79%, 89%, and 96% after RAW264.7 cell incubation with 75 μM TIZ for 3, 6, 9, and 12 h, respectively. As shown in Fig. 3a, d, e, and g, the protein p62 expression level significantly decreased in dose- and time-dependent manners with the TIZ-treated group compared with the control group ($P < 0.01$), This result further indicated that TIZ induced excessive autophagy in the RAW264.7 cells. Autophagosome in cells was examined by TEM to observe autophagy activation induced by TIZ. As shown in Fig. 3h, the control group displayed few autophagosomes and lysosomes in the RAW264.7 cells, whereas many autophagosomes were found in the TIZ-treated group.

As the active prodrug of TIZ, whether NTZ activated autophagy in the RAW264.7 cells should also be investigated. As shown in Fig. 4, the levels of the autophagy proteins LC3 and P62 were examined via Western blot analysis. Compared with the control groups, the LC3-II/LC3-I expression level ratio significantly increased ($P < 0.01$) in dose-dependent manner with NTZ treatment, while p62 expression significantly decreased ($P < 0.01$).

LC3-II/LC3-I expression level ratios in Vero, HepG2, 293T, and RAW264.7 cells

Whether TIZ can activate autophagy in different cell lines were investigated through Western blot by detecting the activation of TIZ on LC3 expression in the Vero, HepG2 and 293T cells. As shown in Fig. 5, compared with the control groups, the LC3-II/LC3-I expression level ratios of the Vero, HepG2, 293T, and RAW264.7 cells significantly increased ($P < 0.01$) after the cells were treated with 50 μM TIZ for 12 h.

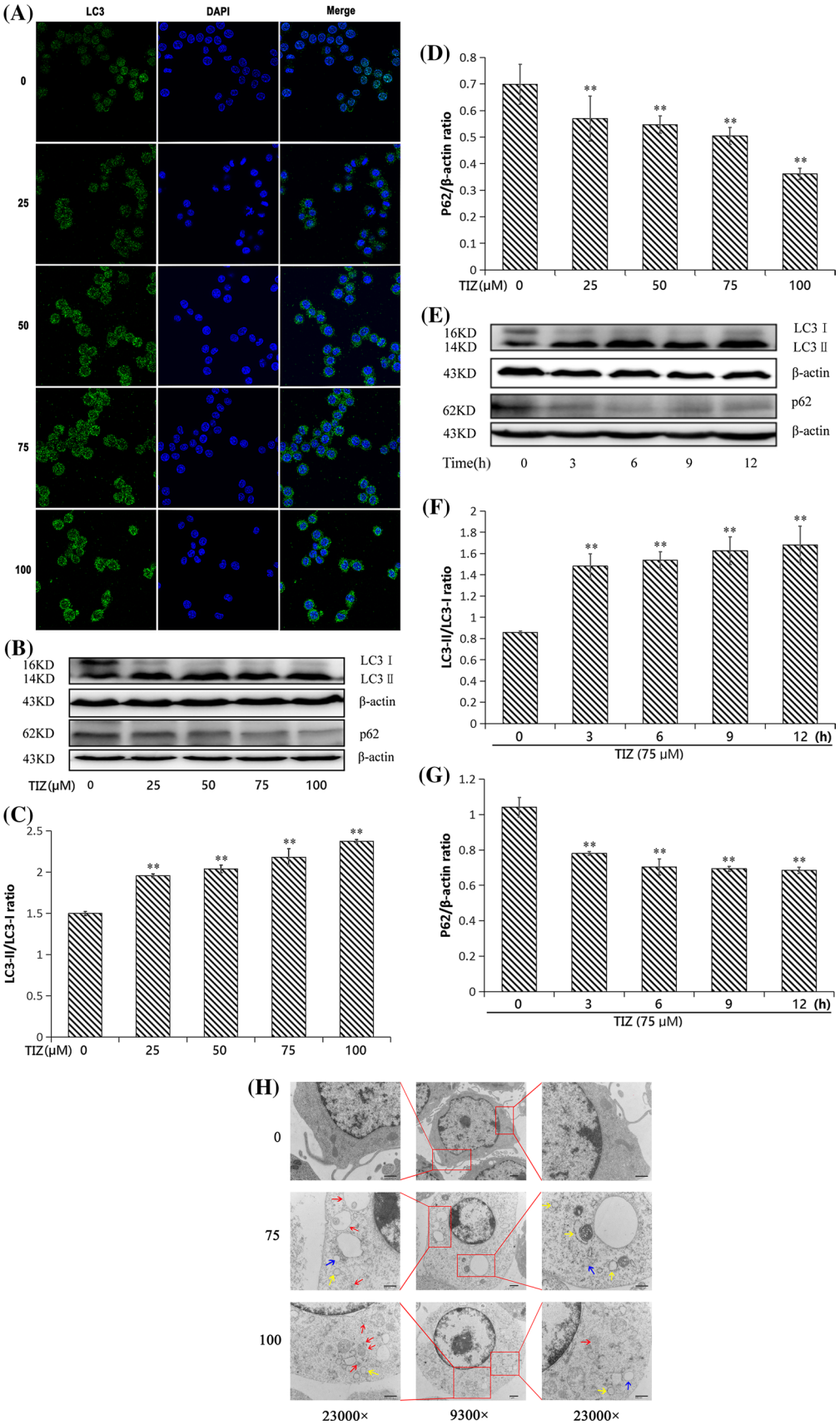
(A)
LC3
DAPI
Merge
0
25
50
75
100
(B)
16KD
14KD
LC3 Ⅰ
LC3 Ⅱ
43KD
β-actin
62KD
p62
43KD
β-actin
TIZ(μM) 0 25 50 75 100
(C)
LC3-II/LC3-I ratio
TIZ(μM) 0 25 50 75 100
(D)
P62/β-actin ratio
TIZ(μM) 0 25 50 75 100
(E)
16KD
14KD
LC3 Ⅰ
LC3 Ⅱ
43KD
β-actin
62KD
p62
43KD
β-actin
Time(h) 0 3 6 9 12
(F)
LC3-II/LC3-I ratio
0 3 6 9 12 (h)
TIZ (75 μM)
(G)
P62/β-actin ratio
0 3 6 9 12 (h)
TIZ (75 μM)
(H)
0
75
100
23000×
9300×
23000×

◂ **Fig. 3** Effects of TIZ on the autophagy of RAW264.7 cells. Note: **a** LC3 and DAPI immunofluorescence staining were performed to detect autophagy in RAW264.7 cells treated with 0, 25, 50, 75 and 100 μM TIZ; **b** a dose-dependent manner of LC3 and p62 was determined in RAW264.7 cells treated with 0, 25, 50, 75 and 100 μM TIZ by western blot; **c** the density analysis of blots of LC3 treated with TIZ; **d** the density analysis of blots of p62 treated with TIZ; **e** a time-dependent manner of LC3 and p62 were determined in RAW264.7 cells treated with 75 μM TIZ by western blot; **f** The density analysis of blots of LC3 treated with different times; G: The density analysis of blots of p62 treated with different times; **h** electron micrographs of morphological changes in RAW264.7 cells treated with 0, 75 and 100 μM TIZ. Phagophore were pointed out by yellow arrows, autophagosomes were pointed out by red arrows, while typical autolysosomes were indicated with blue arrows. Values are expressed as mean ± S.D. of three replicates. $^{**}P < 0.01$ versus the control group

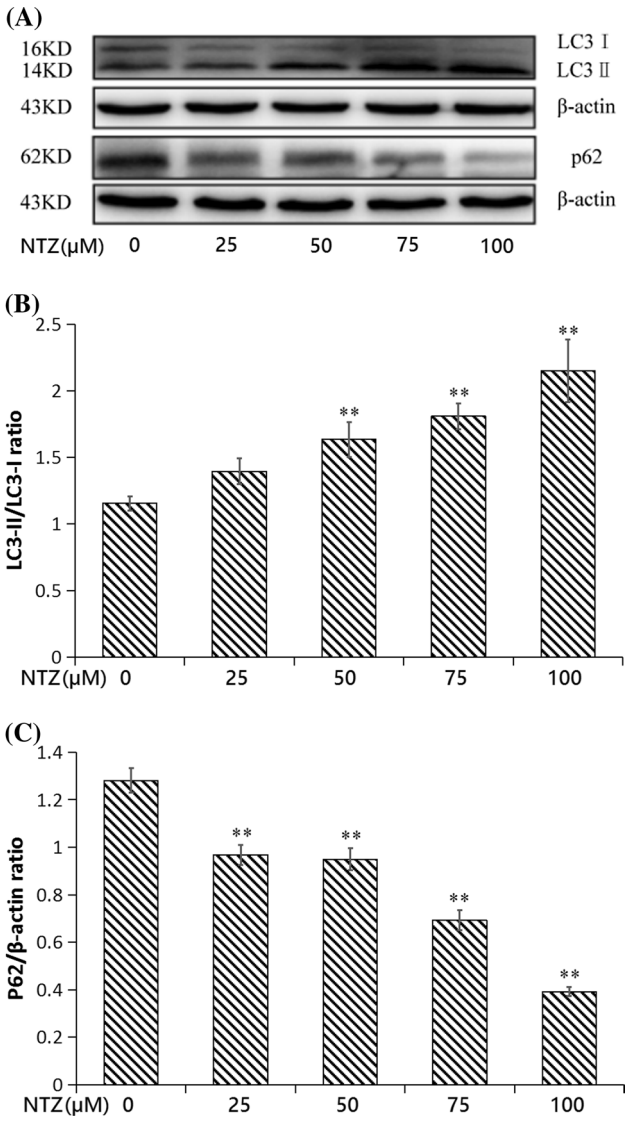

Fig. 4 NTZ induced the autophagy of RAW264.7 cells in dose dependent manner. *Note* **a** a dose-dependent manner of LC3 and p62 was determined in RAW264.7 cells treated with 0, 25, 50, 75 and 100 μM NTZ by western blot; **b** the density analysis of blots of LC3 treated with NTZ; **c** the density analysis of blots of p62 treated with NTZ. Values are expressed as mean ± S.D. of three replicates. $^{**}P < 0.01$ versus the control group

Autophagy-related protein expression level

TIZ-induced autophagy in the RAW264.7 cells was observed, and then the autophagy-related proteins, such as Atg7, Atg5–Atg12 conjugation, and Beclin-1, which were involved in modulating autophagy, were further detected by Western blot. As shown in Fig. 6, the protein expression levels of Beclin-1, Atg7, and Atg5–Atg12 conjugation in the TIZ treatment groups were remarkably higher than those of the control group ($P < 0.05$ or 0.01) and exerted evident

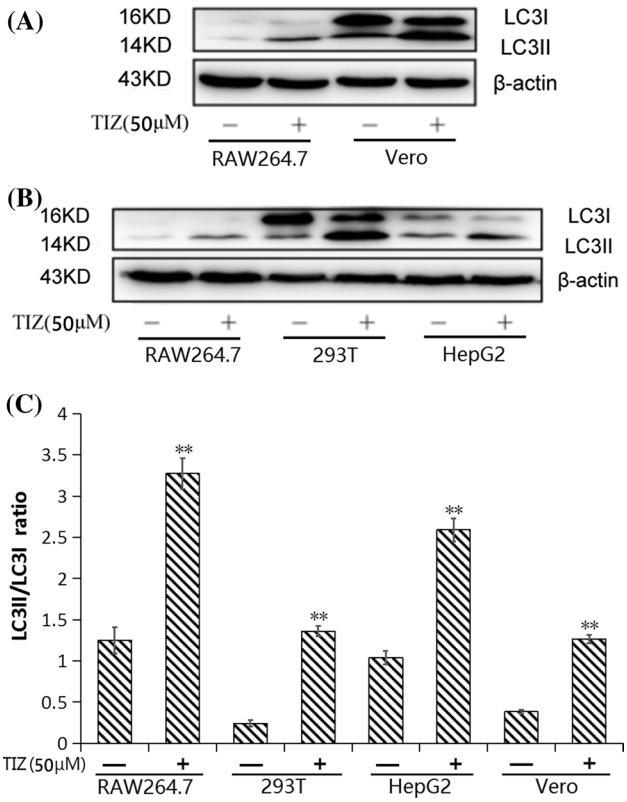

Fig. 5 TIZ activated LC3-II accumulation in Vero, HepG2 and 293T cells. Note: **a**, **b** The expression levels of LC3-II/LC3-I were detected by western blot when each cells treated with 0 and 50 μM TIZ; **c** the ratios analysis of LC3-II/LC3-I treated with TIZ in each cells. Values are expressed as mean ± S.D. of three replicates. $^{**}P < 0.01$ versus the control group

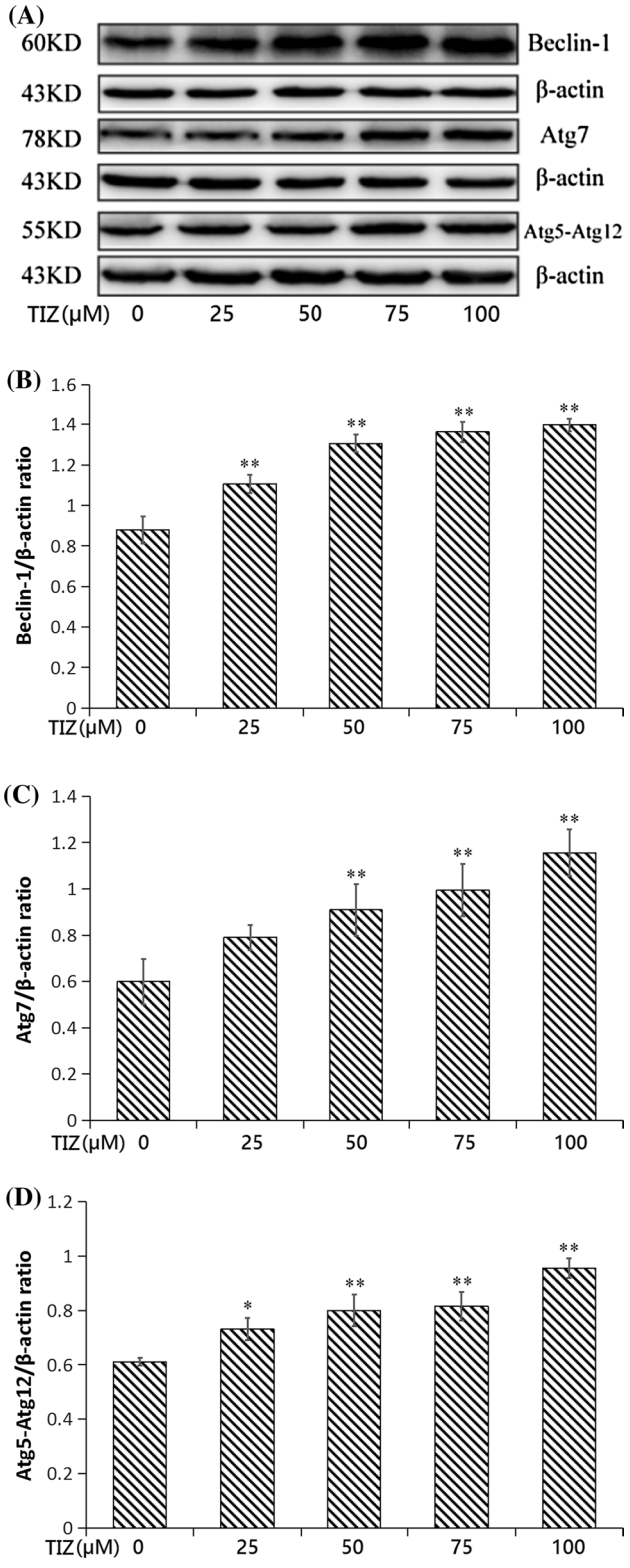

Fig. 6 Effects of TIZ on the expression of autophagy-related proteins. Note: **a** a dose-dependent manner of Beclin-1, Atg7 and Atg5–Atg12 conjugation was determined in RAW264.7 cells treated with 0, 25, 50, 75 and 100 μM TIZ by western blot; **b** the density analysis of blots of Beclin-1 treated with TIZ; **c** the density analysis of blots of Atg7 treated with TIZ; **d** the density analysis of blots of Atg5–Atg12 conjugation treated with TIZ. Values are expressed as mean ± S.D. of three replicates. *$P < 0.05$, **$P < 0.01$ versus the control group

dose-dependent manner. After the RAW264.7 cells were incubated with 100 μM of TIZ for 12 h, the expression levels of Beclin-1, Atg7, and Atg5–Atg12 conjugation significantly increased by 59%, 93%, and 57%, respectively, compared with those of the control group.

PI3K/Akt/mTOR pathway analysis

To determine whether PI3K/Akt/mTOR signaling is involved in TIZ-induced autophagy, we determined the expression levels of the key proteins in PI3K/AKt/mTOR pathway on key protein expression by Western blot after the RAW264.7 cells were treated with TIZ. As shown in Fig. 7a–e, the p-PI3K/PI3K, p-Akt/Akt, p-mTOR/mTOR, and p-ULK1/ULK1 ratios were significantly inhibited upon 25 to 100 μM TIZ treatment for 12 h in a dose-dependent manner ($P < 0.05$ or 0.01). Compared with the control group, the p-PI3K/PI3K, p-Akt/Akt, p-mTOR/mTOR, and p-ULK1/ULK1 ratios in the RAW264.7 cells treated with 100 μM TIZ significantly decreased by 65%, 48%, 40%, and 24%, respectively. Meanwhile, the p-mTOR/mTOR ratio significantly decreased in a time-dependent manner ($P < 0.05$ or 0.01) when the cells were treated with 75 μM TIZ (Fig. 7f and g), thereby further indicating that TIZ repressed the mTOR activity in the RAW264.7 cells.

Detection of PI3K and mTOR inhibitor function

To confirm the role of PI3K/Akt/mTOR pathways on the TIZ-induced autophagy further, we detected the key protein expression levels of the RAW264.7 cells by immunofluorescence staining and Western blot after the cells were pretreated with LY294002 (PI3K inhibitor, 5 μM) or rapamycin (mTOR inhibitor, 1 μM) for 1 h and then to treatment with 75 μM TIZ for 12 h. As shown in Fig. 8a, the RAW264.7 cells of the control and LY294002-treated groups exhibited the negative pattern of the LC3 immunoreactivity in immunofluorescence. However, the RAW264.7 cells exposed to TIZ, rapamycin, and TIZ + rapamycin were observed that the typical cytoplasmic LC3 punctate was significant formed, and LC3-labeled aggregation and the number of the cells with LC3-punctated foci significantly increased. The immunoreactivity intensity of the TIZ + LY294002-treated group was higher than those of the control and LY294002 groups but lower than those of the TIZ, rapamycin, and TIZ + rapamycin groups. Meanwhile, compared with the 75 μM TIZ group, the ratios of p-PI3K/PI3K and LC3-II/LC3-I treated by TIZ + LY294002 and those of p-PI3K/PI3K and p-mTOR/mTOR treated by TIZ + rapamycin were significantly suppressed ($P < 0.05$ or 0.01). However, the ratios of LC3-II/LC3-I treated by TIZ + rapamycin significantly increased ($P < 0.01$) are shown in Fig. 8b–e.

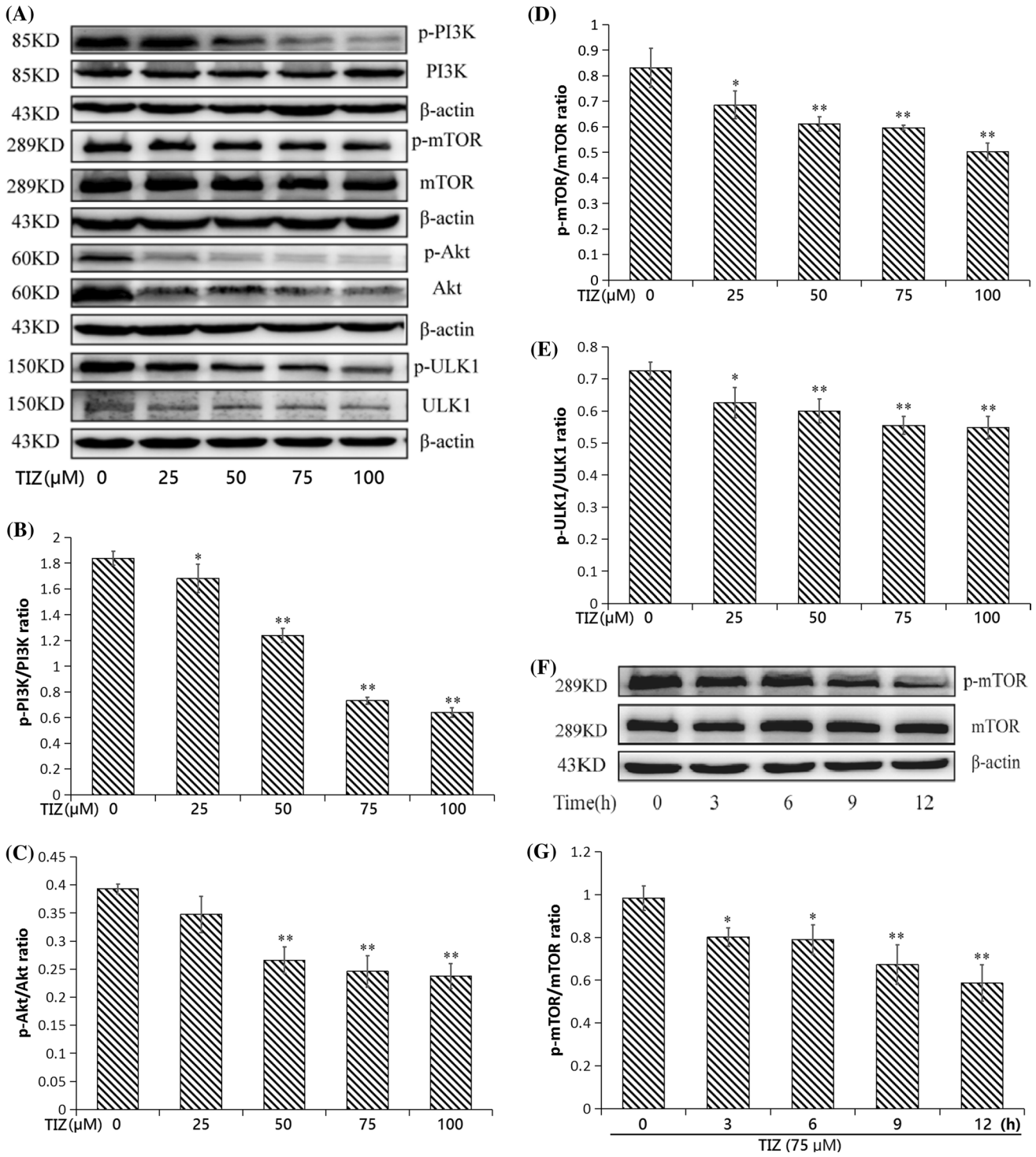

Fig. 7 TIZ suppressed the activation of PI3K/AKT/mTOR pathway. Note: **a** the expression levels of p-PI3K/PI3K, p-Akt/Akt, p-mTOR/mTOR and p-ULK1/ULK1 were detected by western blot when RAW264.7 cells treated with 0, 25, 50, 75 and 100 μM TIZ; **b** the ratios analysis of p-PI3K/PI3K treated with TIZ; **c** the ratios analysis of p-Akt/Akt treated with TIZ; **d** the ratios analysis of p-mTOR/mTOR treated with TIZ; **e** the ratios analysis of p-ULK1/ULK1 treated with TIZ. Values are expressed as mean ± S.D. of three replicates. $^{*}P < 0.05$, $^{**}P < 0.01$ versus the control group

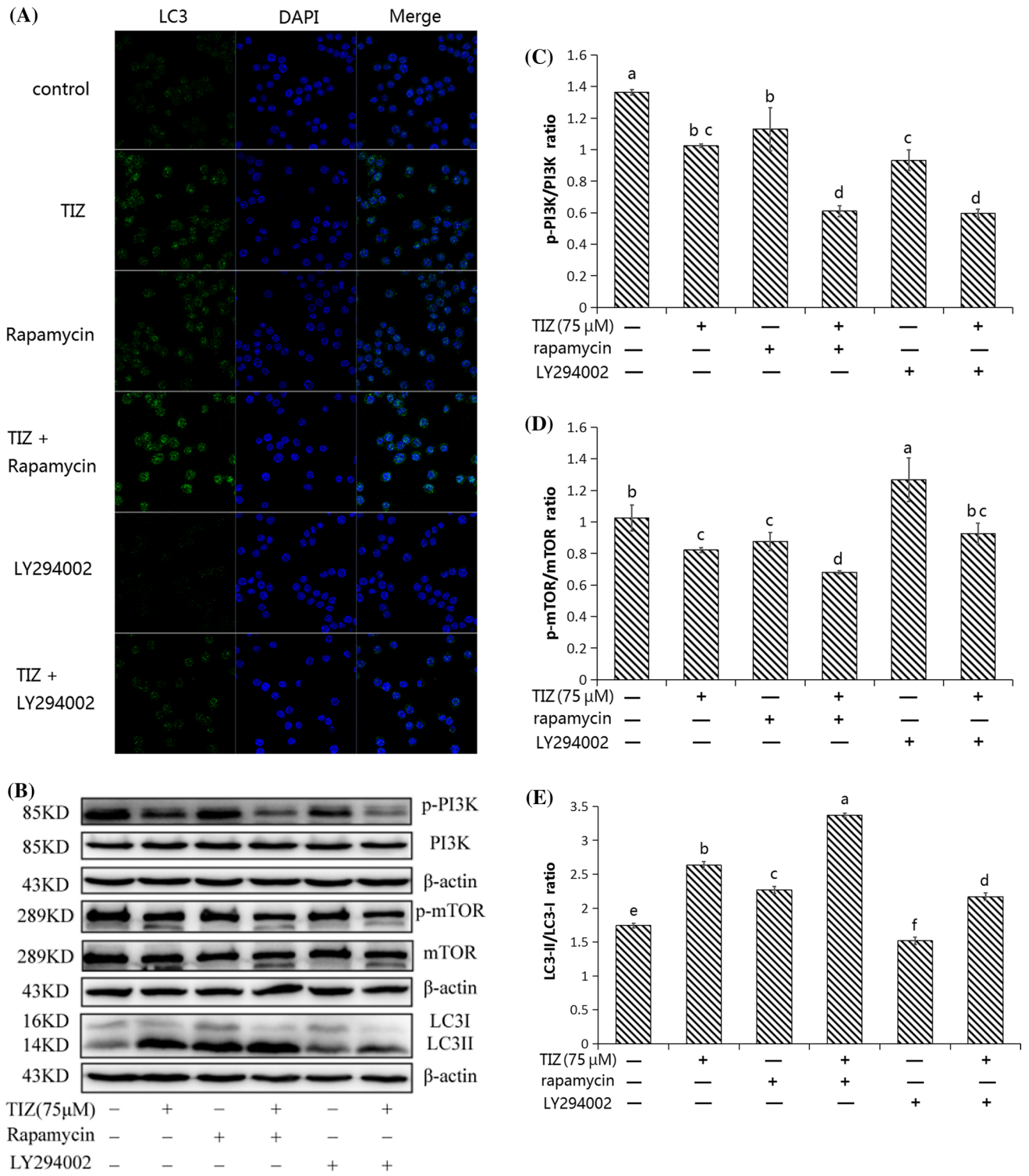

Fig. 8 TIZ-induced autophagy was attenuated by LY294002 and enhanced by rapamycin Note: **a** LC3 and DAPI immunofluorescence staining were performed to detect autophagy in RAW264.7 cells; **b** the expression levels of p-PI3K/PI3K, p-mTOR/mTOR and LC3-II/LC3-I were detected by western blot; **c** the ratios analysis of p-PI3K/PI3K; **d** the ratios analysis of p-mTOR/mTOR; **e** the ratios analysis of LC3-II/LC3-I. TIZ + LY294002 and TIZ + rapamycin mean the cells were pre-treated with LY294002 (PI3K inhibitor, 5 μM) or rapamycin (mTOR inhibitor, 1 μM) then to treatment with 75 μM TIZ for 12 h. Values are expressed as mean ± S.D. of three replicates. Data within a column without the same superscript letters differ significantly ($P < 0.05$ or $P < 0.01$)

Detection of LPS-induced intracellular ROS

DCFH-DA was used to determine the intracellular ROS in the RAW264.7 cells that were treated with LPS. As shown in Fig. 9, the production of the intracellular ROS had significant upregulation after 1.0 μg/mL LPS-treated macrophage. However, the production of the intracellular ROS significantly reduced by 43–79% in a dose-dependent manner ($P < 0.01$), after the LPS-stimulated RAW264.7 cells were incubated with TIZ (25, 50, 75, and 100 μM). TIZ also remarkably suppressed the activation that LPS induced significant increase in the intracellular ROS with increase in the treatment time ($P < 0.01$).

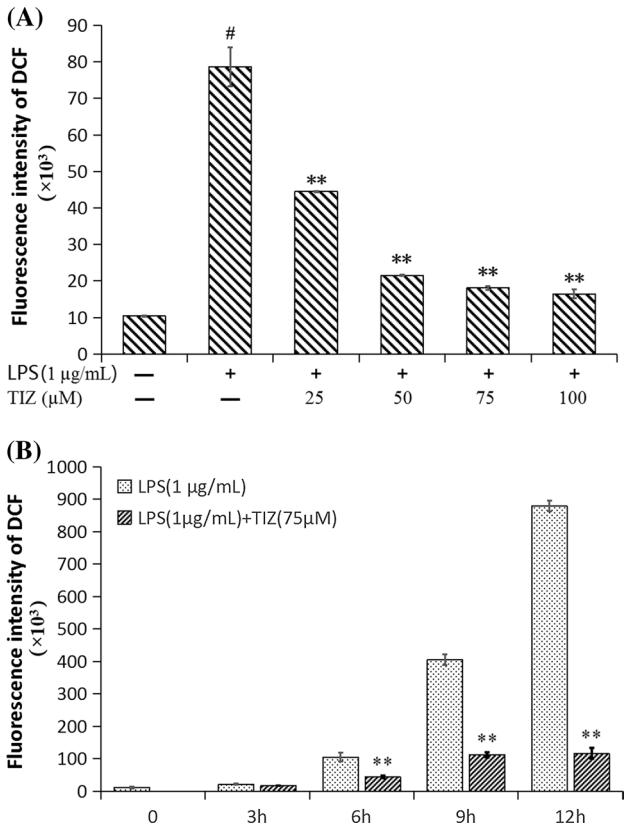

Fig. 9 The fluorescence intensity that intracellular ROS triggered was detected by flow cytometer. Note: **a** the fluorescence intensity was decreased with TIZ concentration increasing. # shows the $P < 0.01$ when single LPS treated group compared with untreated group, and **shows $P < 0.01$ when TIZ groups compared with single LPS treated group. **b** **shows $P < 0.01$ compared between the same treatment groups

Discussion

NTZ exhibits polypharmacology actions via its active metabolite TIZ (Rossignol 2014). Several of the key functional proteins of pathogens (such as PFOR, NQO1) or host cells (such as GSTP1, UPR, PKR, eIF2-α) have been identified as the target of NTZ and TIZ against parasite, anaerobes, and viruses (Hoffman et al. 2007; Müller et al. 2008; Rossignol and Keeffe 2008; Müller and Hemphill 2011; Rossignol 2014). Autophagy and generation of inflammatory response and immune response are directly connected (Peña-Sanoja and De Sanctis 2013; Iida et al. 2017). Drug-induced autophagy can potentially enhance immune responses and provide an attractive therapeutic strategy (Bishop and Bradshaw 2018). However, the effect of the drugs on autophagy in cells has rarely been reported on many molecular mechanisms studies. TIZ inhibits inflammation in murine macrophage in vitro (Shou et al. 2019a) that aroused our interest in exploring the autophagy induced by TIZ in RAW264.7 cells.

Autophagy is an orchestrated homeostatic and catabolic cellular process to dispose of waste material and damaged organelles (Guan et al. 2017). This process also can remove intracellular microbial pathogens and plays an important role in innate and adaptive immunity, cell survival and death, metabolism, and development (Kroemer and Jäättelä, 2005). In monitoring autophagy, the contents of LC3 are proportional to the number of autophagic vacuoles and have been considered to be autophagosome markers in mammals (Tanida et al. 2004). p62 can be used as an autophagy marker because autophagy deficiency can increase p62 level (Manley et al. 2013). In the present study, the results showed that the number of cytoplasmic LC3 punctate cells and the ratio of LC3-II/LC3-I expression significantly increased, and the p62 expression level decreased in dose- and time-dependent manners in the Raw264.7 cells exposed to TIZ compared with the controls. These results indicated that TIZ induced a notable autophagy of Raw264.7 cells. TEM observation showed that the increased number of autophagic vacuoles in the cytoplasm of Raw264.7 cells in the treated groups supported the findings above. TIZ also activated the LC3-II/LC3-I expression level ratios significantly increased in the Vero, HepG2 and 293T cells. The results indicated that TIZ induced evident autophagy not only in Raw264.7 cells but also in other different cell lines. NTZ, as the active prodrug of TIZ, activated the changes in LC3-II/LC3-I and p62 expression levels. The results indicated that leading to

autophagy should be a potential characteristic of thiazolide derivative.

Atg5, Atg7, and Atg12 are key proteins involved in the extension of the phagophoric membrane in autophagic vesicles. The extension process requires the covalent attachment of the protein Atg12 to Atg5 through an ubiquitin-like conjugation system and is activated by Atg7 (Wesselborg and Stork, 2015). Meanwhile, Beclin-1, which is also named Atg6, is a well-known key regulator of autophagy (Wirawan et al. 2012). The expression of Atg5–Atg12 conjugation, Atg7, and Beclin-1 showed significant dose dependent increase with TIZ in the present study. This result indicated that the autophagic structures were formed, and the autophagy membranes extended in the Raw264.7 cells. The results further showed that TIZ induced marked autophagy in the Raw264.7 cells.

The PI3K/Akt/mTOR pathway exhibits an important function in the regulation of autophagy (Zhao et al. 2016). The increase in the expression levels of the autophagy-related proteins (Atg5–Atg12 and Atg7) showed that autophagy levels enhance when the PI3K/Akt/mTOR pathway is inhibited (Xue et al. 2017). Through a Beclin-1-dependent pathway, the activated Akt also induces autophagy (Hanahan and Weinberg 2011). The kinase mammalian target of rapamycin (mTOR) is also a downstream target of the PI3K and kinase Akt pathways, which are activated by the receptors of neurotrophins and growth factors, and promotes cell growth, differentiation, and survival (Heras-Sandoval et al. 2014; Manning and Toker 2017). The mTOR is a pivotal negative regulatory axis of autophagy and direct inhibitors of mTOR and those of pathways activating mTOR subsequently induce autophagy (Cuyàs et al. 2014). To gain insight into the mechanism of TIZ-induced autophagic activity, we examined the PI3K/Akt/mTOR signaling pathway by Western blot assay. The results showed that the expression levels of phosphorylated PI3K, Akt, and mTOR in the Raw264.7 cells exposed to TIZ significantly decreased in a dose-dependent manner. TIZ also significantly decreased the phosphorylated mTOR expression levels in a time-dependent manner. The results indicated that TIZ downregulated PI3K, Akt, and mTOR activity in the Raw264.7 cells. ULK1 is also homologous to Atg1 in yeast and an important protein in autophagy for mammalian cells (Cheong et al. 2011) The suppression of mTOR can induce ULK1 activation through the phosphorylation of ULK1 and ULK1-dependent autophagy (Kim et al. 2011). Therefore, the ULK1 expression level was determined after TIZ exposure in vitro. The phosphorylation of ULK1 was downregulated by TIZ, which also indicated that TIZ induced autophagy through the PI3K/Akt/mTOR pathway. The inhibition of PI3K with LY294002 can also inhibit autophagic sequestration (Blommaart et al. 1997), but the inhibition of mTOR with rapamycin can promote it (Heras-Sandoval et al. 2014). In the present study, the results showed that the LC3 activity was significantly promoted in immunofluorescence and blot assay, and the phosphorylation levels of PI3K and mTOR significantly decreased during the presence of mTOR inhibitor. However, the activity of LC3-II and the phosphorylation of PI3K were suppressed, and the phosphorylation of mTOR was elevated with the presence of PI3K inhibitor. These results indicated that TIZ repressed the activity of the PI3K/Akt/mTOR pathway in the Raw264.7 cells.

Meanwhile, LPS triggers inflammatory response and leads to excessive ROS in immune cells (Park et al. 2015). TIZ represses LPS-induced oxidative stress (Shou et al. 2019a) and inflammatory by inhibiting the NF-κB and MAPK signaling pathways (Shou et al. 2019b). Whether ROS participate in autophagy regulation is unclear, although several compounds can induce autophagy via oxidative stress (Chen et al. 2016). In the present study, the production of intracellular ROS in LPS-treated cells was remarkably repressed by TIZ in the present experiment, thereby indicating that intracellular ROS did not participate in TIZ-induced autophagy in Raw264.7 cells, and the protective effect of TIZ on cells can be multifaceted.

This study was the first to determine that TIZ triggered autophagy through a mechanism that was involved in the repression of PI3K/AKT/mTOR pathway in the RAW264.7 murine macrophages (Fig. 10). The results provide novel insights into the protection of TIZ on cells. This work also displayed that thiazolide compounds can be a new autophagy inducer and inhibitor of PI3K/AKT/mTOR family molecule. Further studies are warranted to explore the potential mechanism for the complex biological targets and functions, such as through autophagy, antioxidant, and anti-inflammatory activities, of TIZ.

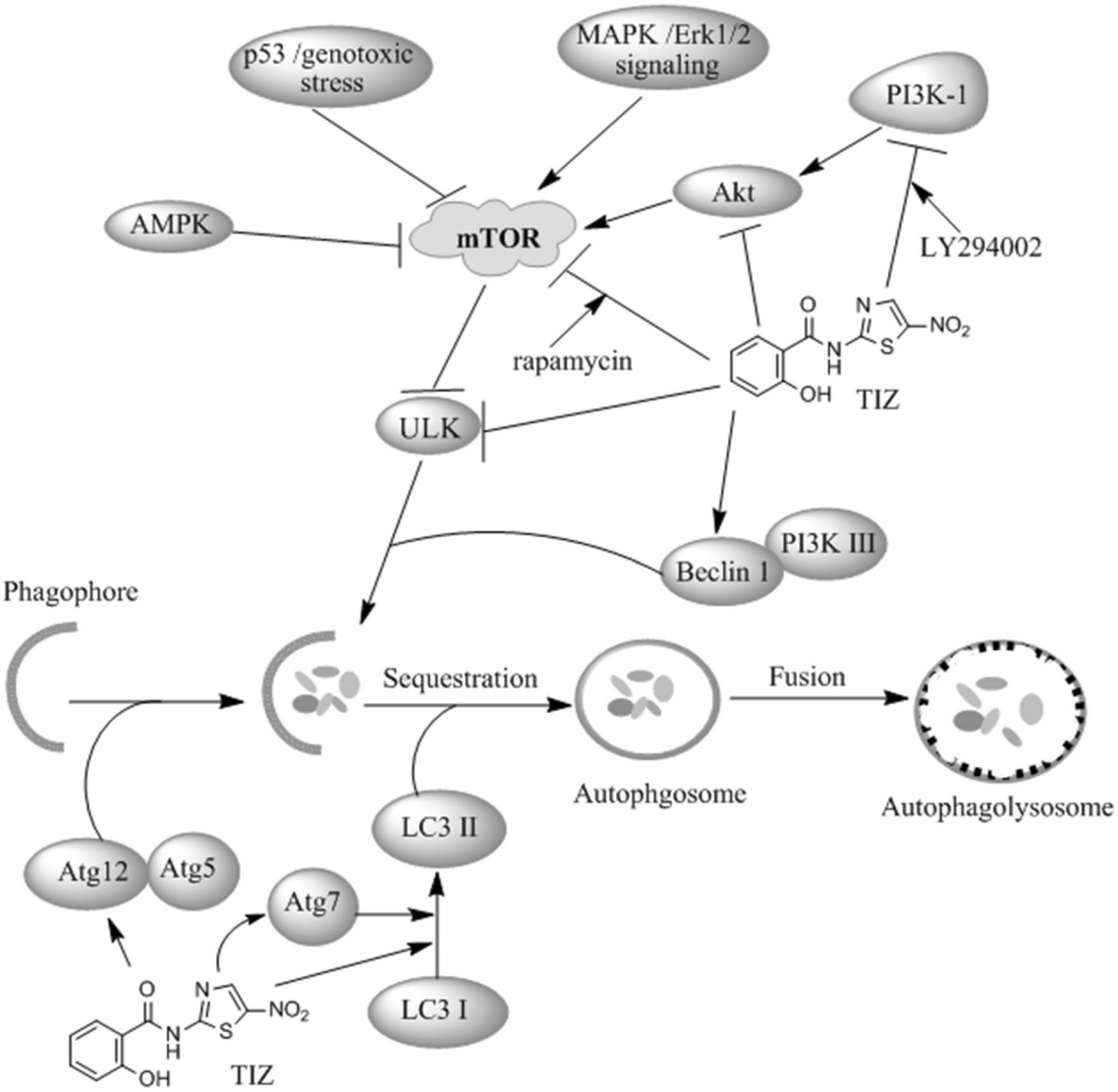

Fig. 10 In the proposed model of the molecular mechanism of TIZ-induced autophagy. Note: The inducing functions have been shown through inactivating Beclin-1, Atg7 and Atg5–Atg12 conjugation, and inhibiting p-PI3K/PI3K, p-Akt/Akt, p-mTOR/mTOR and p-ULK1/ULK1. ← means activation; ⊥means inhibition

Acknowledgements This work was financially supported by the National Natural Science Foundation of China (Grant No. 31872516). This project was also supported in part by the National Key Technology Research and Development Program of China (Grant No. 2015BAD11B00) and the National Key Research and Development Program of China (Grant No. 2018YFD0500302). We are also extremely grateful to Mr. Shi of the Central Laboratory of SHVRI for his assistance in electron microscopy research.

Compliance with ethical standards

Conflict of interest The authors declare that they have no conflict of interest.

References

Adagu IS, Nolder D, Warhurst DC, Rossignol JF (2002) In vitro activity of nitazoxanide and related compounds against isolates of *Giardia intestinalis, Entamoeba histolytica*, and *Trichomonas vaginalis*. J Antimicrob Chemother 49:103–111. https://doi.org/10.1093/jac/49.1.103

Belardo G, Cenciarelli O, La Frazia S, Rossignol JF, Santoro MG (2015) Synergistic effect of nitazoxanide with neuraminidase inhibitors against influenza A viruses in *vitro*. Antimicrob Agents Chemother 59:1061–1069. https://doi.org/10.1128/AAC.03947-14

Bishop E, Bradshaw TD (2018) Autophagy modulation: a prudent approach in cancer treatment? Cancer Chemother Pharmacol 82(6):913–922. https://doi.org/10.1007/s00280-018-3669-6

Blommaart EF, Krause U, Schellens JP, Vreeling-Sindelárová H, Meijer AJ (1997) The phosphatidylinositol 3-kinase inhibitors

wortmannin and LY294002 inhibit autophagy in isolated rat hepatocytes. Eur J Biochem 243(1–2):240–246. https://doi.org/10.1111/j.1432-1033.1997.0240a.x

Chen Z, Liu X, Ma S (2016) The roles of mitochondria in autophagic cell death. Cancer Biother Radiopharm 31(8):269–276. https://doi.org/10.1089/cbr.2016.2057

Cheong H, Lindsten T, Wu J, Lu C, Thompson CB (2011) Ammonia-induced autophagy is independent of ULK1/ULK2 kinases. Proc Natl Acad Sci USA 108(27):11121–11126. https://doi.org/10.1073/pnas.1107969108

Cuyàs E, Corominas-Faja B, Joven J, Menendez JA (2014) Cell cycle regulation by the nutrient-sensing mammalian target of rapamycin (mTOR) pathway. Methods Mol Biol 1170:113–144. https://doi.org/10.1007/978-1-4939-0888-2_7

Dubreuil L, Houcke I, Mouton Y, Rossignol JF (1996) In vitro evaluation of activities of nitazoxanide and tizoxanide against anaerobes and aerobic organisms. Antimicrob Agents Chemother 40:2266–2270

Essick EE, Sam F (2010) Oxidative stress and autophagy in cardiac disease, neurological disorders, aging and cancer. Oxid Med Cell Longev 3(3):168–177. https://doi.org/10.4161/oxim.3.3.12106

Fox LM, Saravolatz LD (2005) Nitazoxanide: a new thiazolide antiparasitic agent. Clin Infect Dis 40(8):1173–1180. https://doi.org/10.1086/428839

Guan H, Piao H, Qian Z, Zhou X, Sun Y, Gao C, Li S, Piao F (2017) 2,5-Hexanedione induces autophagic death of VSC41 cells via a PI3K/Akt/mTOR pathway. Mol Biosyst 13(10):1993–2005. https://doi.org/10.1039/c7mb00001d

Hanahan D, Weinberg RA (2011) Hallmarks of cancer: the next generation. Cell 144(5):646–674. https://doi.org/10.1016/j.cell.2011.02.013

Heras-Sandoval D, Pérez-Rojas JM, Hernández-Damián J, Pedraza-Chaverri J (2014) The role of PI3K/AKT/mTOR pathway in the modulation of autophagy and the clearance of protein aggregates in neurodegeneration. Cell Signal 26(12):2694–2701. https://doi.org/10.1016/j.cellsig.2014.08.019

Hoffman PS, Sisson G, Croxen MA, Welch K, Harman WD, Cremades N, Morash MG (2007) Antiparasitic drug nitazoxanide inhibits the pyruvate oxidoreductases of *Helicobacter pylori*, selected anaerobic bacteria and parasites, and *Campylobacter jejuni*. Antimicrob Agents Chemother 51(3):868–876. https://doi.org/10.1128/AAC.01159-06

Iida T, Onodera K, Nakase H (2017) Role of autophagy in the pathogenesis of inflammatory bowel disease. World J Gastroenterol 23(11):1944–1953. https://doi.org/10.3748/wjg.v23.i11.1944

Kim J, Kundu M, Viollet B, Guan KL (2011) AMPK and mTOR regulate autophagy through direct phosphorylation of Ulk1. Nat Cell Biol 13(2):132–141. https://doi.org/10.1038/ncb2152

Kimura T, Takabatake Y, Takahashi A, Isaka Y (2013) Chloroquine in cancer therapy: a double-edged sword of autophagy. Cancer Res 73(1):3–7. https://doi.org/10.1158/0008-5472.CAN-12-2464

Kobayashi S (2015) Choose delicately and reuse adequately: the newly revealed process of autophagy. Biol Pharm Bull 38(8):1098–1103. https://doi.org/10.1248/bpb.b15-00096

Kroemer G, Jäättelä M (2005) Lysosomes and autophagy in cell death control. Nat Rev Cancer 5(11):886–897. https://doi.org/10.1038/nrc1738

La Frazia S, Ciucci A, Arnoldi F, Coira M, Gianferretti P, Angelini M, Belardo G, Burrone OR, Rossignol JF, Santoro MG (2013) Thiazolides, a new class of antiviral agents effective against rotavirus infection, target viral morphogenesis, inhibiting viroplasm formation. J Virol 87:11096–11106. https://doi.org/10.1128/JVI.01213-13

Lam KK, Zheng X, Forestieri R, Balgi AD, Nodwell M, Vollett S, Anderson HJ, Andersen RJ, Av-Gay Y, Roberge M (2012) Nitazoxanide stimulates autophagy and inhibits mTORC1 signaling and intracellular proliferation of *Mycobacterium tuberculosis*. PLoS Pathog 8:e1002691. https://doi.org/10.1371/journal.ppat.1002691

Levine B, Kroemer G (2008) Autophagy in the pathogenesis of disease. Cell 132(1):27–42. https://doi.org/10.1016/j.cell.2007.12.018

Li JJ, Tang Q, Li Y, Hu BR, Ming ZY, Fu Q, Qian JQ, Xiang JZ (2006) Role of oxidative stress in the apoptosis of hepatocellular carcinoma induced by combination of arsenic trioxide and ascorbic acid. Acta Pharmacol Sin 27(8):1078–1084. https://doi.org/10.1111/j.1745-7254.2006.00345.x

Manley S, Williams JA, Ding WX (2013) Role of p62/SQSTM1 in liver physiology and pathogenesis. Exp Biol Med (Maywood) 238(5):525–538. https://doi.org/10.1177/1535370213489446

Manning BD, Toker A (2017) AKT/PKB signaling: navigating the network. Cell 169(3):381–405. https://doi.org/10.1016/j.cell.2017.04.001

Müller J, Hemphill A (2011) Identification of a host cell target for the thiazolide class of broad-spectrum anti-parasitic drugs. Exp Parasitol 128(2):145–150. https://doi.org/10.1016/j.exppara.2011.02.007

Müller J, Sidler D, Nachbur U, Wastling J, Brunner T, Hemphill A (2008) Thiazolides inhibit growth and induce glutathione-S-transferase Pi (GSTP1)-dependent cell death in human colon cancer cells. Int J Cancer 123(8):1797–1806. https://doi.org/10.1002/ijc.23755

Park J, Min JS, Kim B, Chae UB, Yun JW, Choi MS, Kong IK, Chang KT, Lee DS (2015) Mitochondrial ROS govern the LPS-induced pro-inflammatory response in microglia cells by regulating MAPK and NF-κB pathways. Neurosci Lett 584:191–196. https://doi.org/10.1016/j.neulet.2014.10.016

Peña-Sanoja MJ, De Sanctis JB (2013) Autophagy and immune response. Invest Clin 54(3):325–337

Rossignol JF (2014) Review: nitazoxanide: a first-in-class broad-spectrum antiviral agent. Antivir Res 110:94–103. https://doi.org/10.1016/j.antiviral.2014.07.014

Rossignol JF, Keeffe EB (2008) Thiazolides: a new class of drugs for the treatment of chronic hepatitis B and C. Future Microbiol 3(5):539–545. https://doi.org/10.2217/17460913.3.5.539

Rossignol JF, La Frazia S, Chiappa L, Ciucci A, Santoro MG (2009) Thiazolides, a new class of anti-influenza molecules targeting viral hemagglutinin at the post-translational level. J Biol Chem 284:29798–29808. https://doi.org/10.1074/jbc.M109.029470

Shou J, Cheng X, Wang X, Xue F, Wang M, Liu Y, Fei C, Zhang L, Zhang K, Li J (2019a) Effects of tizoxanide on oxidative stress and inflammatory cytokine on lipopolysaccharide induced in raw264.7 cells. Chin J Anim Infect Dise. 27(2):71–77

Shou J, Kong X, Wang X, Tang Y, Wang C, Wang M, Zhang L, Liu Y, Fei C, Xue F, Li J, Zhang K (2019b) Tizoxanide inhibits inflammation in LPS activated RAW264.7 macrophages via the suppression of NF-κB and MAPKs activation. Inflammation 42(4):1336–1349. https://doi.org/10.1007/s10753-019-00994-3

Somvanshi VS, Ellis BL, Hu Y, Aroian RV (2014) Nitazoxanide: nematicidal mode of action and drug combination studies. Mol Biochem Parasitol 193:1–8. https://doi.org/10.1016/j.molbiopara.2013.12.002

Sotthibundhu A, McDonagh K, von Kriegsheim A, Garcia-Munoz A, Klawiter A, Thompson K, Chauhan KD, Krawczyk J, McInerney V, Dockery P, Devine MJ, Kunath T, Barry F, O'Brien T, Shen S (2016) Rapamycin regulates autophagy and cell adhesion in induced pluripotent stem cells. Stem Cell Res Ther 7(1):166. https://doi.org/10.1186/s13287-016-0425-x

Sparrer KMJ, Gableske S, Zurenski MA, Parker ZM, Full F, Baumgart GJ, Kato J, Pacheco-Rodriguez G, Liang C, Pornillos O, Moss J, Vaughan M, Gack MU (2017) TRIM23 mediates virus-induced autophagy via activation of TBK1. Nat Microbiol 2(11):1543–1557. https://doi.org/10.1038/s41564-017-0017-2

Stachulski AV, Pidathala C, Row EC, Sharma R, Berry NG, Iqbal M, Bentley J, Allman SA, Edwards G, Helm A, Hellier J, Korba BE, Semple JE, Rossignol JF (2011) Thiazolides as novel antiviral agents. 1. Inhibition of hepatitis B virus replication. J Med Chem 54:4119–4132. https://doi.org/10.1021/jm200153p

Stachulski AV, Swift K, Cooper M, Reynolds S, Norton D, Slonecker SD, Rossignol JF (2017) Synthesis and pre-clinical studies of new amino-acid ester thiazolide prodrugs. Eur J Med Chem 126:154–159. https://doi.org/10.1016/j.ejmech.2016.09.080

Stockis A, Aleemon AM, De Bruyn S, Gengler C (2002a) NTZ pharmacokinetics and tolerability in man using single ascending oral doses. Int J Clin Pharmacol Ther 40:213–220. https://doi.org/10.5414/cpp40213

Stockis A, De Bruyn S, Gengler C, Rosillon D (2002b) Nitazoxanide pharmacokinetics and tolerability in man during 7 days dosing with 0.5 g and 1.0 g b.i.d. Int J Clin Pharmacol Ther 40:221–227. https://doi.org/10.5414/cpp40221

Tanida I, Ueno T, Kominami E (2004) LC3 conjugation system in mammalian autophagy. Int J Biochem Cell Biol 36(12):2503–2518. https://doi.org/10.1016/j.biocel.2004.05.009

Wesselborg S, Stork B (2015) Autophagy signal transduction by ATG proteins: from hierarchies to networks. Cell Mol Life Sci 72(24):4721–4757. https://doi.org/10.1007/s00018-015-2034-8

Wirawan E, Lippens S, Vanden Berghe T, Romagnoli A, Fimia GM, Piacentini M, Vandenabeele P (2012) Beclin1: a role in membrane dynamics and beyond. Autophagy 8(1):6–17. https://doi.org/10.4161/auto.8.1.16645

Wu H, Ding J, Li S, Lin J, Jiang R, Lin C, Dai L, Xie C, Lin D, Xu H, Gao W, Zhou K (2019) Metformin promotes the survival of random-pattern skin flaps by inducing autophagy via the AMPK-mTOR-TFEB signaling pathway. Int J Biol Sci 15(2):325–340. https://doi.org/10.7150/ijbs.29009

Xue JF, Shi ZM, Zou J, Li XL (2017) Inhibition of PI3K/AKT/mTOR signaling pathway promotes autophagy of articular chondrocytes and attenuates inflammatory response in rats with osteoarthritis. Biomed Pharmacother 89:1252–1261. https://doi.org/10.1016/j.biopha.2017.01.130

Ylä-Anttila P, Vihinen H, Jokitalo E, Eskelinen EL (2009) Monitoring autophagy by electron microscopy in Mammalian cells. Methods Enzymol 452:143–164. https://doi.org/10.1016/S0076-6879(08)03610-0

Zhang Q, Sun J, Wang Y, He W, Wang L, Zheng Y, Wu J, Zhang Y, Jiang X (2017) Antimycobacterial and anti-inflammatory mechanisms of baicalin via induced autophagy in macrophages infected with *Mycobacterium tuberculosis*. Front Microbiol 8:2142. https://doi.org/10.3389/fmicb.2017.02142

Zhao ZQ, Yu ZY, Li J, Ouyang XN (2016) Gefitinib induces lung cancer cell autophagy and apoptosis via blockade of the PI3K/AKT/mTOR pathway. Oncol Lett 12(1):63–68. https://doi.org/10.3892/ol.2016.4606